

Supercritical CO₂ impregnation of α-tocopherol into PET/PP films for active packaging applications

Paola Franco, Loredana Incarnato, Iolanda De Marco*

Department of Industrial Engineering, University of Salerno,

Via Giovanni Paolo II, 132, 84084, Fisciano (SA), Italy

*idemarco@unisa.it Fax: +39-89-964057

Abstract

Supercritical carbon dioxide impregnation technique was used to adsorb α-tocopherol (TOC), a natural antioxidant, on monolayer and multilayer polyethylene terephthalate (PET)/polypropylene (PP) films to obtain active packaging. Supercritical impregnation experiments were performed at 17 MPa and 40 °C using different supports: PP films, PET films (ut-PET), corona discharge treated PET surface (ct-PET) films, PET/PP films. Supercritical carbon dioxide (SC-CO₂) impregnation revealed to be an effective technique in the attainment of active packaging films. Indeed, very high amounts of TOC were impregnated (up to 3.2 mg_{TOC}/cm²_{film} considering a monolayer PP film and up to 2.66 mg_{TOC}/cm²_{film} considering a multilayer film). Field emission scanning electron microscopy (FESEM) showed how the impregnation with TOC modified the film surface (which became heterogeneous). Fourier transform infrared spectroscopy (FT-IR) revealed the presence in the impregnated films of both TOC and polymers characteristic bands. Differential scanning calorimetry (DSC) indicated that the presence of SC-CO₂ induced a slight reduction in the crystallinity percentage of the polymers. Moreover, migration of α-tocopherol from the packaging films in a food simulant was studied using UV–vis spectroscopy, and the effectiveness of the supercritical impregnation to obtain the controlled-release of the active agent was verified. Finally,

- 23 antioxidant activity tests confirmed the preservation of TOC antioxidant power after its
- 24 impregnation on monolayer and multilayer films.
- 25 Keywords: PET/PP multilayer film; supercritical impregnation; migration tests; antioxidant activity.

26 **1. Introduction**

27 In recent years, the development of advanced packaging solutions gained considerable attention
28 to prolong food shelf-life and preserve its quality and safety. One of the most attractive strategies
29 turned out to be the active packaging, which provides the controlled release of antioxidant or
30 antimicrobial agents included in some kinds of active packaging [1-4]. The active packaging is
31 considered an effective response against lipid oxidation [5], which is one of the key causes of food
32 deterioration.

33 A monolayer or a multilayer film containing the antioxidant can constitute the active packaging. In
34 particular, a multilayer can consist of two layers (i.e., outer layer and active matrix layer) or of four
35 layers (i.e., outer layer, barrier layer, active layer and control/inner layer) [5, 6]. Briefly, the barrier
36 layer is placed between the outer layer and the active layer, and it allows to reduce the undesired
37 migration of the active agent towards the outside of the package. The active layer, instead,
38 incorporates the active compound. If a four-layer film is used, the inner layer, directly joined to the
39 active layer, permits to control the active agent's migration towards the food surface.

40 Active packaging films can be carried out through many conventional techniques, such as
41 extrusion or solvent casting, and the active agent can be contained into the plastic film or coated
42 onto it. Up to now, different routes were attempted to reach the controlled-release of the active
43 compound, as, for example, its incorporation into porous matrices [7, 8] or its encapsulation in a
44 polymeric shell [9-12]. However, traditional methods for active packaging production have some
45 drawbacks, mainly the deterioration of the active agent due to the high temperatures used during
46 the process, that can also lead to the partial volatilization of the active compound with the solvent
47 used. As a result, low penetration of the active agent in the polymer substrate and reduced
48 loading efficiencies are generally obtained [13, 14]. An alternative solvent-free process is the
49 impregnation using supercritical carbon dioxide (SC-CO₂) [15, 16] since it is possible to operate at

50 low-temperature thanks to SC-CO₂ mild critical conditions ($T_c=31.1$ °C, $P_c=7.38$ MPa) [17, 18]. SC-
51 CO₂ allows solubilizing and, then, incorporating different kinds of organic compounds into polymer
52 matrices because it has high diffusivity and acts as a plasticizing and a swelling agent for polymers
53 [19]. However, the impregnation of a specific compound into a polymer matrix is strongly affected
54 by the interaction between an active solute/SC-CO₂/polymer substrate [19].

55 In the last few years, some articles were published on this subject, showing the effectiveness of
56 the supercritical impregnation for food packaging applications [14, 20-24]. For example,
57 Milovanovic et al. [14] loaded thymol into poly(lactic acid) (PLA)/poly(ϵ -caprolactone) (PCL) films
58 obtaining a strong bactericidal action against *Escherichia coli* and *Bacillus subtilis*. Villegas et al.
59 [22] impregnated cinnamaldehyde, a flavonoid present in the cinnamon essential oil, into PLA
60 films. The loaded films exhibited good antibacterial activity and excellent thermal and mechanical
61 properties, considering that they showed higher flexibility and greater resistance with respect to
62 the unprocessed PLA films. Belizón et al. [23] produced active multilayer polyethylene
63 terephthalate (PET)/polypropylene (PP) films containing antioxidant mango polyphenols. The
64 latter two polymers are among the most commonly used ones for the development of active
65 packaging [25]; the active films obtained by Belizón et al. [23] through supercritical impregnation
66 preserved foods from degradation over an extended period. The same multilayer substrate was
67 chosen by Cejudo Bastante et al. [24] that studied the supercritical impregnation of caffeic acid
68 and of an olive leaf extract in PET/PP films, evaluating the antioxidant activity using the DPPH
69 assay. In that paper, the potential of supercritical impregnation was highlighted, as well as the
70 difficulty of optimizing the operating conditions of the process because of the numerous variables,
71 often linked one to each other.

72 Categorized as GRAS (“Generally Recognized As Safe”) by the US Food and Drug Administration, α -
73 tocopherol (TOC) was widely proposed as a natural antioxidant for the production of controlled-

74 release packaging [7, 8, 26-29], in order to reduce food oxidation, but also as a stabilizer for
75 polymer processing [5]. For example, Chen et al. [28] used the cast film extrusion to produce
76 ethylene vinyl alcohol and low-density polyethylene films containing 1500 ppm tocopherol and
77 1500 ppm quercetin, for the long-term inhibition of lipid oxidation; whereas, Hwang et al. [30]
78 added TOC and resveratrol at various concentrations ($0.01-0.04 \text{ mg}_{\text{antioxidant}}/\text{mg}_{\text{film}}$) to PLA film by a
79 melt compounding and compression molding process for packaging applications. On the other
80 hand, to our knowledge, there are no studies in the literature on supercritical impregnation of TOC
81 for these purposes (reduction of food oxidation and stabilizing polymer processing), although it
82 was applied in other fields, such as pharmaceutical one [31, 32]. For example, De Marco and
83 Reverchon [31] impregnated TOC into maize starch aerogel to enhance the vitamin bioavailability,
84 improving its dissolution rate, whereas Yokozaki and Shimoyama [32] loaded TOC into silicone
85 aerogel to reduce the diffusivity of timolol maleate, an ocular drug used in the treatment of
86 glaucoma.

87 This work aims at obtaining an active packaging, using SC-CO₂ that incorporates TOC in multilayer
88 PET/PP films. To optimize the active packaging, a comparison between a film in which TOC is
89 impregnated on the surface of untreated PET (ut-PET) and a film in which TOC is adsorbed on the
90 surface of PET subjected to corona discharge treatment (ct-PET) was performed. The confirmation
91 of the attainment of an active agent controlled-release system was given by migration tests in
92 food simulant and by the antioxidant activity quantification.

93 **2. Materials and methods**

94 *2.1 Materials*

95 Ethanol (EtOH, purity 99.9 %) and α -tocopherol (TOC, purity 96%) were purchased by Carlo Erba
96 (Cornaredo, MI, Italy) and Sigma-Aldrich (Milan, Italy), respectively. Morlando Group S.r.l. (Naples,

97 Italy) supplied carbon dioxide (CO₂, purity 99 %) . The distilled water was obtained using a
98 laboratory water distiller, purchased by ISECO S.p.A. (Aosta, Italy).

99 Bi-oriented Polyethylene Terephthalate (PET) film, with 23 μm thickness, was supplied by Nuroll
100 S.p.a. Polypropylene (PP) film, with 33 μm thickness, was provided by Ifis S.p.A (Marcianise, Italy).

101 Multilayer PET/PP films were obtained by lamination technique, joining the single layers PP and
102 PET films through the two-component polyurethane solvent based adhesive Polurene FP44A/58-
103 01, supplied by Sapici S.p.a (Cernusco sul Naviglio, Italy), with an application weight of 3 g/m² by
104 dry content. For the preparation of multilayer films, both monolayer PET and PP films were
105 subjected to corona discharge treatment on the surface, to obtain sufficient wettability and
106 adhesion capability [33]. The obtained multilayer film has a thickness of approximately 60 μm.

107 *2.2 Corona discharge treatment*

108 A corona discharge treatment was carried out in line during the film production. The treatment
109 was applied to PET films (and to one side of the PP film when the multilayer film has to be
110 prepared). Briefly, the electric discharge causes the oxidation of the polymeric surface through
111 the generation of free radicals, resulting in the formation of additional polar groups on the surface
112 that involve a strong adhesion of adhesives, dyes, coatings, etc. [33, 34]. It is worth noting that this
113 treatment acts on small depths (nanometers) of the treated surface conferring it the desired
114 properties, but leaving the bulk properties of the polymer unchanged.

115 High voltage and frequency discharge (corona discharge) were applied at atmospheric pressure
116 with two treater machines, operating at a maximum output power of 8 kW set at an operating
117 power of 3 kW to ensure a surface tension of 55 dyne/cm.

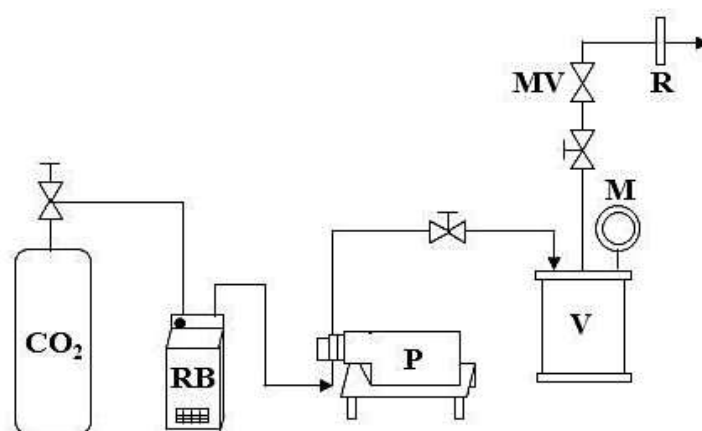
118 *2.3 Apparatus and procedure for supercritical impregnation*

119 The impregnation tests were performed employing a laboratory-scale apparatus (in Figure 1),
120 which consists in a cylindrical stainless steel autoclave (NWA GmbH, Lorrach, Germany) with an
121 internal volume of 100 mL, closed with two clamps on the top and the bottom. CO₂ was slowly fed
122 at a constant flow rate (10 g/min) through a high-pressure pump (Milton Roy, mod. Milroyal B,
123 Pont-Saint-Pierre, France), whose head was cooled by a refrigerating bath (Julabo, Seelbach,
124 Germany). When the working pressure was reached, the operating conditions were maintained for
125 a fixed time. An impeller, located on the top cap and driven by a variable velocity electric motor,
126 ensured good stirring. Thin band heaters were used to heat the autoclave, whose internal
127 temperature was measured by a K-type thermocouple (accuracy ± 0.1 °C). The thermal control was
128 guaranteed by a PID controller (Watlow, mod. 93, Toledo, OH, USA), whereas pressure was
129 measured by a digital manometer (Parker, Minneapolis, MN, USA). A micrometric valve (Hoke,
130 mod. 1315G4Y, Spartanburg, SC, USA), preceded by an on/off valve, allowed a slow
131 depressurization. Through a rotameter at the exit of the cylinder, it was possible to evaluate the
132 CO₂ flow rate .

133 Impregnation experiments were carried out using a static method [35, 36]. A small film piece
134 (about 2.5 cm x 2.5 cm) was accurately weighed and put in a small stainless steel container,
135 packed into filter paper (to avoid its contact with the liquid TOC); then, the sample was placed on
136 the bottom of the cylindrical autoclave. In particular, the weights of PP and PET monolayer films
137 were respectively 23.5 ± 1.5 mg and 24.5 ± 2.5 mg, whereas, for the multilayers PET/PP film, they
138 were in the range 45.0 ± 3.0 mg. A weighed amount of TOC approximately equal to 0.80 g,
139 corresponding to its saturation concentration in SC-CO₂ at the given pressure and temperature (10
140 mg_{TOC}/g_{CO2}) [31], was instead placed inside a small opened container, coaxially located on the
141 impeller, to allow its contact with SC-CO₂. The chosen pressure assured a high solubility of TOC in

142 SC-CO₂ [31]. The amount of CO₂ inside the cylinder, which was about 80.8 g, was calculated from
143 its density value at the operating temperature and pressure. Carbon dioxide density was evaluated
144 using the Bender equation of state [37]. Once the autoclave was closed, CO₂ was slowly delivered
145 to the cylinder and simultaneously heated up to the required temperature. When the desired
146 pressure (17 MPa) was reached, CO₂ flow was stopped, and the operating conditions were
147 maintained for a fixed time. At the end of the experiment, the autoclave was depressurized with a
148 constant flow rate (about 0.1 MPa/min). Once the depressurization ended, the loaded film was
149 recovered and weighed. The weight increase of the sample was related to the quantity of
150 impregnated TOC, which was also checked using UV/vis spectrophotometer, as reported below in
151 the analytical methods section. In order to assure that the impregnated films did not contain
152 adsorbed carbon dioxide in the polymer, each loaded sample was weighted an hour after the end
153 of the experiment. Impregnation tests were repeated twice; the difference in weight between the
154 experiments conducted at the same operating conditions was less than 5%.

155 Impregnation kinetics were determined to find out the time required by TOC to reach the
156 equilibrium concentration at the chosen value of temperature and pressure. Kinetic data were
157 obtained at different contact times (2- 48 h), at 17 MPa and 40 °C.



158

159 Figure 1 Schematic representation of the impregnation laboratory plant. CO₂: carbon dioxide supply; RB: refrigerating
160 bath; P: pump; V: vessel; M: manometer; MV: micrometric valve; R: rotameter.

161 *2.4 Analytical methods*

162 Films were observed by Field Emission Scanning Electron Microscopy (FESEM, mod. LEO 1525, Carl
163 Zeiss SMT AG, Oberkochen, Germany) before and after impregnation of TOC with SC-CO₂. Small
164 film pieces were placed on a carbon tab previously attached to an aluminum stub (Agar Scientific,
165 Stansted, United Kingdom) and, then, covered with gold-palladium (layer thickness 250 Å) using a
166 sputter coater (mod. 108 A, Agar Scientific, Stansted, United Kingdom). Many FESEM images were
167 taken for each sample to verify its uniformity.

168 Fourier transform infrared (FT-IR) spectra were obtained through an FTIR spectrophotometer
169 (IRTracer100, Shimadzu Italia, Milan, Italy) at a resolution of 0.5 cm⁻¹ in a scan wavenumber range
170 from 4000 to 450 cm⁻¹, as the mean of 16 measurements. Potassium bromide (KBr) was used as an
171 infrared transparent matrix and well-mixed in an agate mortar with small pieces of each film that
172 has to be analyzed. Then, a hydraulic press (gradually increasing the pressure up to 30 MPa)
173 compressed the samples blended with KBr in the form of disks [38].

174 Differential scanning calorimetry (DSC) measurements were carried out by a differential scanning
175 calorimeter (mod. TC11, Mettler-Toledo International Inc., Columbus, OH, USA) using Mettler
176 STARE system. Each film (about 5 mg) was crimped into an aluminum pan. For both PP and PET,
177 the analysis was conducted under a nitrogen gas flow equal to 100 mL/min. PP samples were
178 heated from -35 °C to 200 °C at a rate of 10 °C/min, and then held at 200 °C for 5 min to ensure
179 the complete melting of crystallites. Then, they were cooled from 200 °C to -35 °C at a rate of 10
180 °C/min and, after, heated up again from -35 °C to 200 °C (10 °C/min). To better detect the PP glass
181 transition temperature, DSC was repeated in the range from -50 °C to 20 °C at a rate of 5 °C/min.

182 PET samples were, instead, heated from 25 °C to 300 °C at a rate of 10 °C/min, held at 300 °C for 5
183 min, then cooled from 300 °C to 25 °C (10 °C/min) and finally heated up again from 25 °C to 300 °C
184 (10 °C/min). The glass transition temperature (T_g), the melting temperature (T_m) and the melting
185 enthalpy (ΔH_m) were determined from the second heating scan, according to the ASTM D3418-12
186 method [39]. A comparison with the melting enthalpy of pure crystalline PP and PET (207 J/g and
187 140 J/g, respectively) allowed to calculate the crystallinity degree (%) of pure and loaded films.

188 TOC loadings, evaluated to assess the weight increase of the impregnated samples, and *in vitro*
189 migration studies were performed by a UV/vis spectrophotometer (model Cary 50, Varian, Palo
190 Alto, CA, USA) at a wavelength of 295 nm [28]. Each analysis was repeated twice, and the mean
191 release profiles were proposed in this work, plotting the percentage of released TOC as a function
192 of time.

193 The migration tests were conducted at 40 °C in food simulant D1 (50 % EtOH), according to the
194 European Commission Regulation No. 10/2011 [40]. In detail, small film pieces containing an
195 equivalent amount of TOC (5 mg) were immersed in 70 mL of food simulant D1, continuously
196 stirred at 100 rpm. The absorbance was monitored until the steady state was reached. Then, the
197 maximum absorbance measured at the end of the release; i.e., when the film released all TOC to
198 the outer ethanolic solution, was converted into TOC concentration using a calibration curve,
199 obtained using very diluted standards at different concentrations of TOC in the release medium
200 (0.2850, 0.1425, 0.0713 and 0.0356 mg/mL). In particular, the percentage of TOC released at any
201 time was determined as follows:

$$202 \quad \text{TOC release, \%} = \frac{\text{the amount of TOC measured at a certain time}}{\text{the maximum amount of released TOC}} \times 100 \quad (1)$$

203 To eliminate a possible influence of other polymer additives, release tests were also performed on
204 pure single layer PP and PET films and on multilayer PET/PP films before supercritical
205 impregnation; however, no significant absorbance value was detected at 295 nm.

206 The antioxidant activity of TOC impregnated into the different films was determined using 2,2-
207 diphenyl-1-picrylhydrazyl (DPPH) as stable free radical, according to the method described by
208 Brand-Williams [41]. Tests were carried out in triplicate.

209 Ethanolic solutions at different concentrations of pure TOC (30-800 ppm) were tested. Firstly, 0.1
210 mL of each solution was added to 3.9 mL of a 6×10^{-5} mol/L solution of DPPH. The decrease in the
211 absorbance was monitored using a UV/vis spectrophotometer (model Cary 50, Varian, Palo Alto,
212 CA) at 515 nm (characteristic wavelength of DPPH) every 5 minutes for two hours under dark at
213 room temperature until the steady state was achieved. The initial DPPH concentration was
214 measured at time zero. From these kinetic results, Efficient Concentration (EC_{50}) of TOC; i.e., the
215 concentration of antioxidant that decreased the initial DPPH one by 50%, was graphically
216 calculated and it was found to be equal to 191.3 $\mu\text{g}/\text{mL}$. Moreover, this preliminary study allowed
217 to select the amount of TOC to be considered for the impregnated films analyses to avoid a total
218 reaction of the DPPH and, at the same time, to apply the DPPH protocol optimized for the activity
219 of the impregnated films by Cejudo Bastante et al. [24]. Indeed, the DPPH protocol was slightly
220 modified to evaluate the antioxidant activity of the impregnated films [24]. An amount of sample
221 was submerged in 4 mL of 6×10^{-5} mol/L DPPH in ethanol. The absorbance was measured at 515
222 nm every 5 minutes for two hours under dark at room temperature. To have an accurate
223 comparison, the antioxidant activity tests were performed considering the same amount of TOC
224 (0.7 mg/mL) for all the samples.

225 The percentage inhibition (%I), which represents the amount of DPPH that reacts with a given
226 concentration of TOC, was calculated as follows:

227
$$\%I = \left(1 - \frac{A_i}{A_0}\right) * 100 \quad (2)$$

228 where A_0 is the initial DPPH absorbance at 515 nm and A_i is the final absorbance of each sample
229 measured at 515 nm after two hours of reaction.

230 To ensure that the adhesive or other polymer additives did not distort the measurements of
231 antioxidant activity, a DPPH assay was also performed on the film before impregnation without
232 observing the antioxidant activity.

233 **3. Results and discussion**

234 The work can be divided into four main steps:

235 (1) study of impregnation kinetics of TOC into single layer PET and PP films;

236 (2) single layer loaded films characterization to choose the best conditions to develop active
237 multilayer PET/PP films;

238 (3) study of impregnation kinetics of TOC into multilayer PET/PP film;

239 (4) multilayer PET/PP loaded films characterization to investigate the potential as controlled-
240 release packaging.

241 *3.1 Kinetics of TOC impregnation into single-layer films*

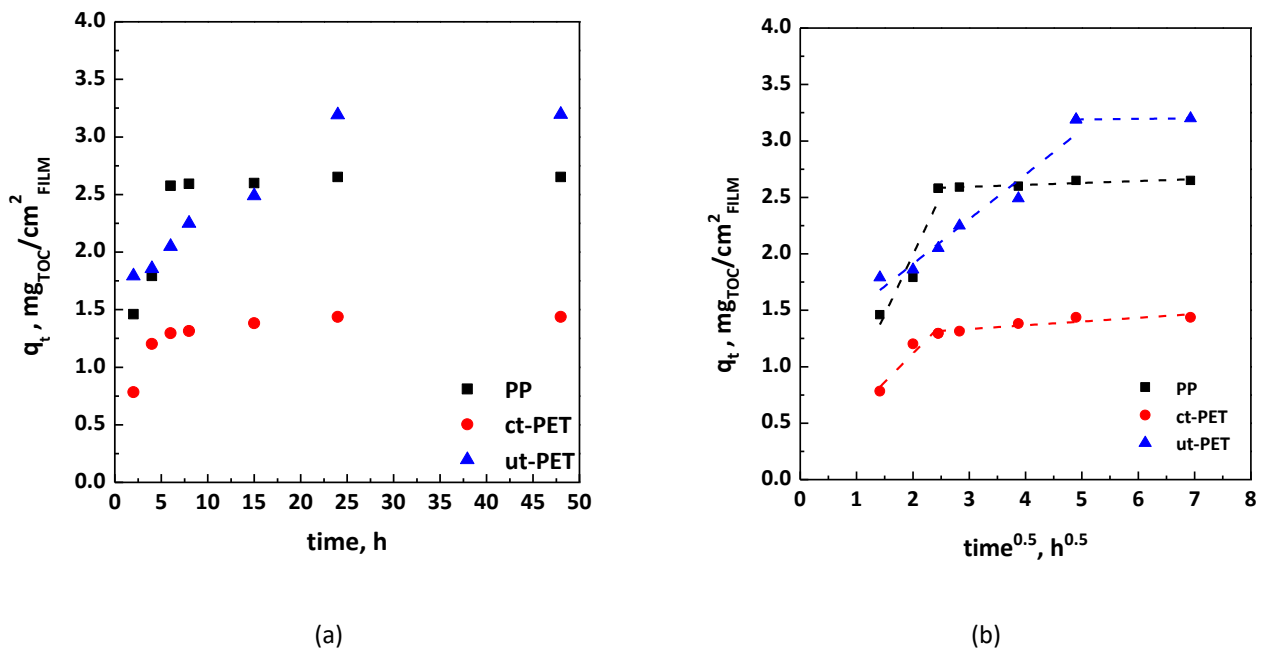
242 Firstly, the impregnation of TOC into single layer films was studied at 17 MPa, 40 °C in
243 correspondence of various contact times (from 2 to 48 h). In particular, the impregnation kinetics
244 of TOC into PP film, on the side of ut-PET and ct-PET were determined and compared, as shown in
245 Figure 2a. Uptake was expressed per unit area of film as q_t ; i.e., mg of impregnated TOC per cm^2 of
246 film ($\text{mg}_{\text{TOC}}/\text{cm}^2_{\text{PP}}$, $\text{mg}_{\text{TOC}}/\text{cm}^2_{\text{ut-PET}}$ and $\text{mg}_{\text{TOC}}/\text{cm}^2_{\text{ct-PET}}$, respectively). From the kinetic curves in
247 Figure 2a, an increase of the loaded TOC can be observed with the increase of contact times, up to
248 a maximum value, which was found at 24 h for all the films. Moreover, comparing the

249 impregnation kinetics obtained for the different substrates, the lowest quantity of impregnated
250 TOC was achieved with ct-PET, whereas the amount of loaded TOC into PP and ut-PET was more
251 similar. TOC uptake is different considering different polymers because swelling capability as well
252 as diffusivity [42] of CO₂ in the matrix vary from polymer to polymer. These properties influenced
253 the amount of an active substance that can be charged into a polymer. As previously discussed,
254 the high-frequency discharge used during the corona treatment causes the formation of additional
255 polar groups on the polymer surface that probably have a weak attraction for fat-soluble TOC,
256 leading to the low penetration of the active compound into the ct-PET surface [33, 34].

257 From a quantitative point of view, it is possible to note that the obtained loading is very high, if
258 compared with literature results [19, 28, 30]; indeed, the amount of loaded TOC, expressed in
259 terms of uptake, reached a very high value equal to 3.20 mg_{TOC}/cm²_{FILM} in case of ut-PET after 24 h
260 of impregnation. This achievement allows to overcome the main drawbacks of conventional
261 techniques used to obtain active packaging; i.e., low penetration into the polymer and low loading
262 efficiencies [19, 28, 30]. The high loadings reached confirmed the potential of the supercritical
263 impregnation of active compounds into polymeric films with loadings greater than the ones
264 obtained in previous papers focused on the same technique; for example, the loading of thymol
265 into PLA/PCL films obtained by Milovanovic et al. [14] was equal to 35.8 wt %. Therefore, the
266 loadings shown in Figure 2a obtained using supercritical impregnation are 2-3 orders of magnitude
267 higher than the values reported in previous works [14, 28]. To determine which is, among “film
268 diffusion” and “intraparticle diffusion”, the limiting step of the process, the adsorption of TOC into
269 the different films were plotted in terms of q_t versus $t^{0.5}$ (Figure 2b), according to the Weber and
270 Morris approach [43]. Indeed, it is well known that q_t vs. $t^{0.5}$ plots can be characterized by a
271 multilinearity, ascribable to the different steps that occur in the adsorption process. It is possible
272 to note from Figure 2b that, for all the films, in correspondence of lower values of $t^{0.5}$, the plot is

273 sharper because of a boundary layer effect due to the adsorption of TOC on the exterior part of
 274 the film: film diffusion is the governing step at the earlier stages of the process. The second part of
 275 the plot is linear and ascribable to the adsorption stage: at these stages, the adsorption is
 276 governed by the intraparticle diffusion.

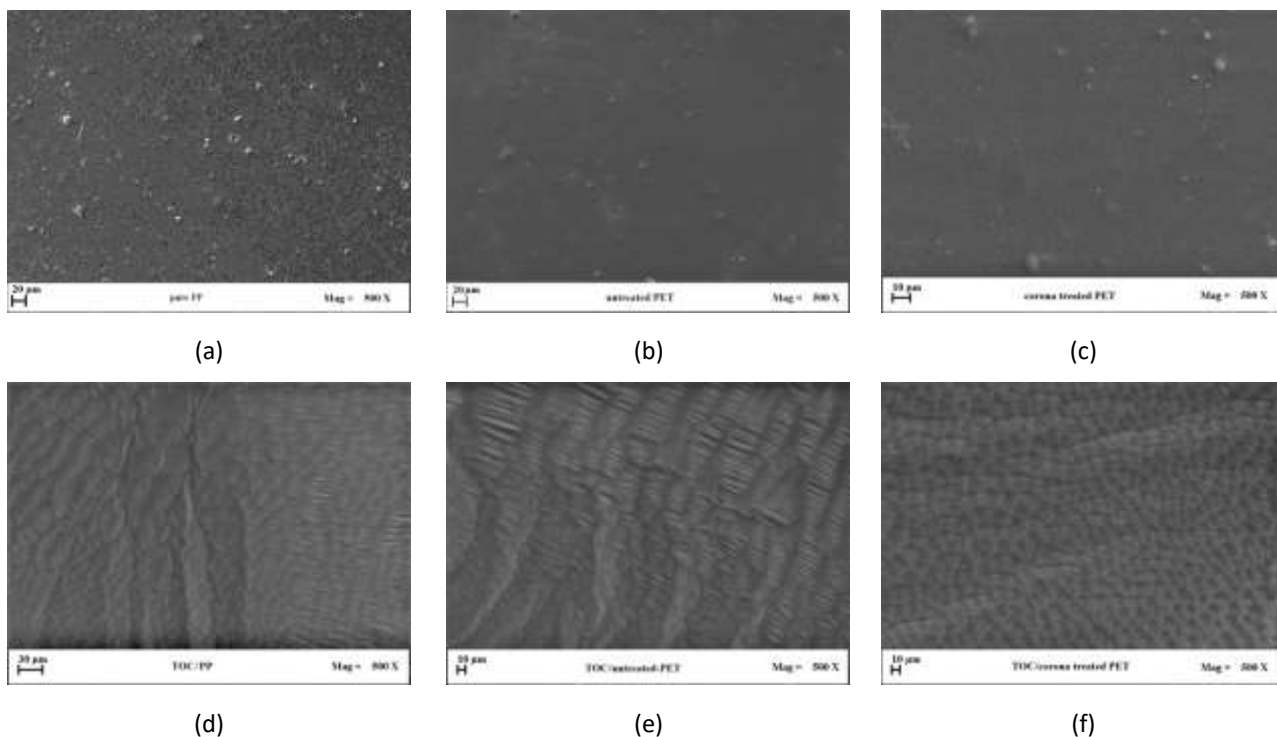
277



278 Figure 2 Impregnation of TOC into PP film, corona discharge treated and untreated surface of PET film: (a) kinetic
 279 curves; (b) intraparticle diffusion plot.

280 3.2 Characterization of single-layer films after impregnation

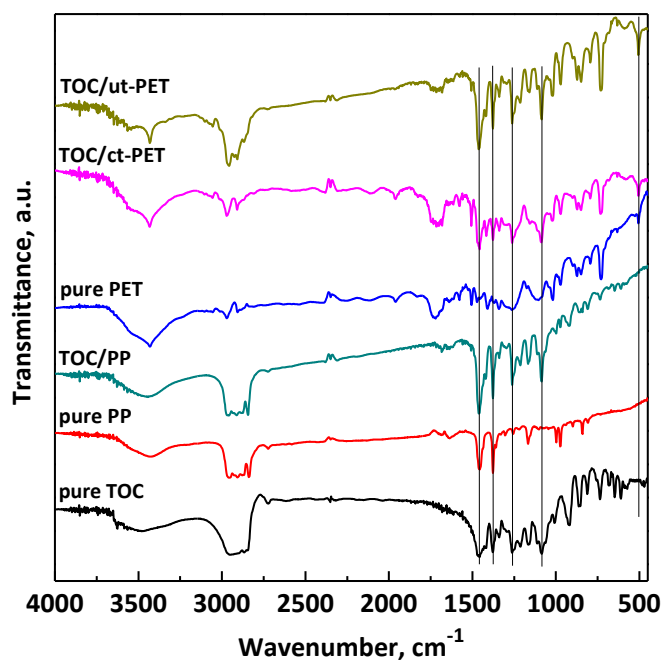
281 FESEM images of films before and after TOC impregnation (17 MPa, 40 °C and 6 h) are reported in
 282 Figure 3 for PP, ut-PET and ct-PET samples. Comparing the FESEM images of the unloaded films
 283 (Fig. 3a, 3b and 3c) with the ones of the impregnated films (Fig. 3d, 3e and 3f), it is possible to
 284 observe that, in the case of the unloaded films, the observed surface is smooth, whereas, in the
 285 case of the impregnated films, the film surfaces appear discontinuous because of the presence of
 286 TOC.



287 Figure 3 FESEM images of films: (a) pure PP; (b) pure ut-PET; (c) pure ct-PET; (d) TOC impregnated in PP; (e) TOC
 288 impregnated in ut-PET; (f) TOC impregnated in ct-PET.

289 FT-IR analyses were performed for pure TOC, pure films, and TOC impregnated into each
 290 monolayer, as reported in Figure 4. The spectra of the impregnated samples exhibited both the
 291 characteristic bands of the polymer and the active compound; in particular, all of them showed
 292 peaks ascribable to TOC at 1262 cm^{-1} for CH_2 and at 1086 cm^{-1} for plane bending of phenyl [44].
 293 The increase of the absorbance peaks at 1378 and 1460 cm^{-1} , related to the methyl symmetric and
 294 asymmetric bending [44], observed in the spectra of all loaded films with respect to the ones of
 295 pure films, confirmed the presence of TOC. Indeed, the percentage increase of the absorbance at
 296 1378 and 1460 cm^{-1} was significant, ranging from 63 % for loaded PP to 91 % for loaded ut-PET in
 297 the case of the first mentioned peak and from 33% for loaded PP to 84% for loaded ut-PET in the
 298 case of the second one. Moreover, an increase of the peak at around 500 cm^{-1} corresponding to
 299 the C-C bending was found in the spectrum of loaded ut-PET.

300



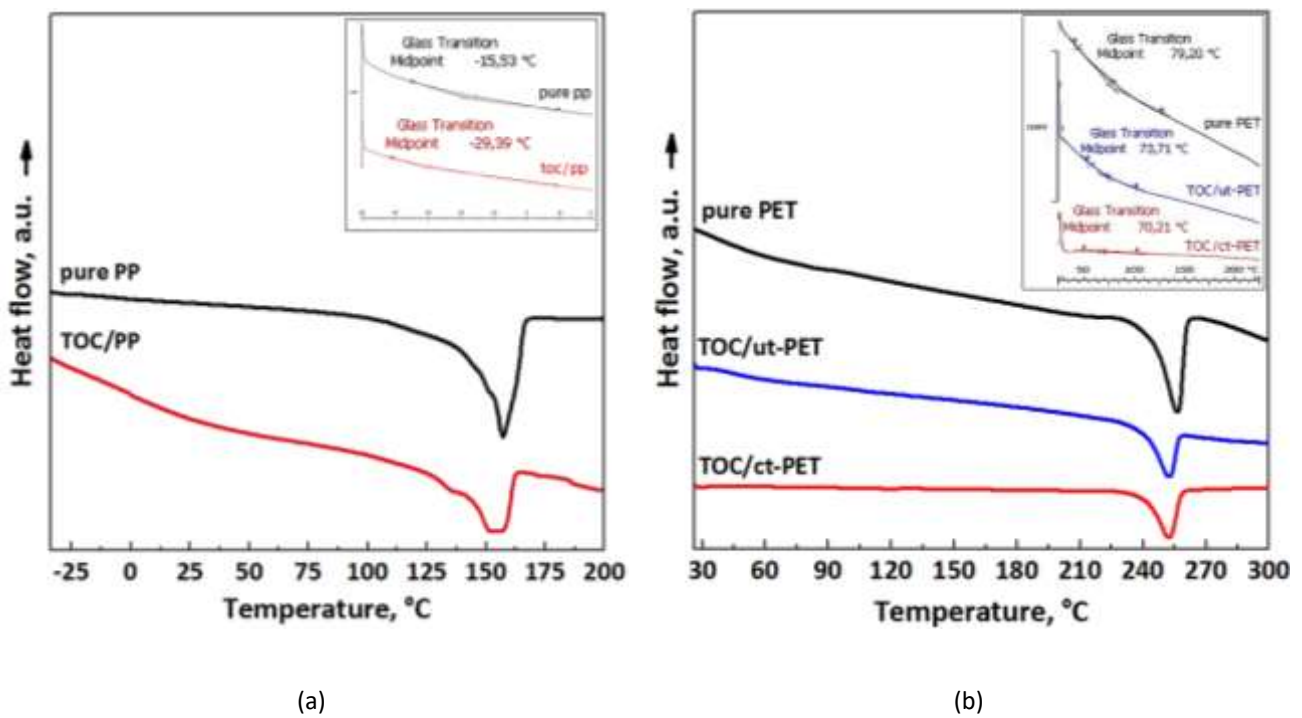
301

302 Figure 4 FT-IR spectra of pure TOC, pure PP and PET films, TOC impregnated into PP, ut-PET and ct-PET. Vertical lines
 303 are referred to the peaks at 1460, 1378, 1262, 1086 and 500 cm^{-1} .

304 Figure 5 showed DSC thermograms of films before and after TOC impregnation (17 MPa, 40 °C and
 305 6 h). In agreement with the literature [45], in Figure 5a it is possible to observe that PP curve
 306 shows a peak at about 157 °C corresponding to its melting temperature, slightly shifted at a lower
 307 temperature after supercritical impregnation. Moreover, the T_g of pure PP was observed at about -
 308 16 °C [46], and it shifted at a lower temperature equal to -29 °C for impregnated PP. In Figure 5b,
 309 the PET curve exhibits a peak at around 256 °C, which corresponds to the T_m , according to
 310 literature data [47]; the T_m slightly shifted at a lower temperature in the case of PET films
 311 processed by supercritical impregnation (ut-PET, ct-PET). The corona discharge treatment does not
 312 influence the thermal properties, being a surface treatment; i.e., it only modifies the film
 313 electrostatic surface charge (and not the bulk properties) [33].

314

315 Moreover, PET thermogram shows a T_g at about 79 °C [47], less prominent and shifted at lower
 316 temperatures in impregnated samples; i.e., about 74 °C for impregnated ut-PET and 70 °C for
 317 impregnated ct-PET. The shifts of melting and glass transition temperatures may be ascribed to
 318 the well-known plasticizing effect of compressed fluids in the presence of semicrystalline polymers
 319 [19, 48]. Moreover, some literature studies show that a plasticizing effect can be also caused by
 320 active substances, including TOC, leading to an improvement in the flexibility and fatigue strength
 321 of polymers [49, 50]. The melting enthalpy (ΔH_m) and the crystallinity degree (%) for pure and
 322 loaded films were reported in Table 1. Comparing the results of pure and impregnated films, it is
 323 possible to observe that the presence of SC-CO₂ induced a slightly reduction in the crystallinity
 324 percentage of the polymers.



325 Figure 5 Entire DSC thermograms and enlargement of a part of curves (with the indication of T_g) for pure and
 326 impregnated films: (a) PP samples; (b) PET samples.

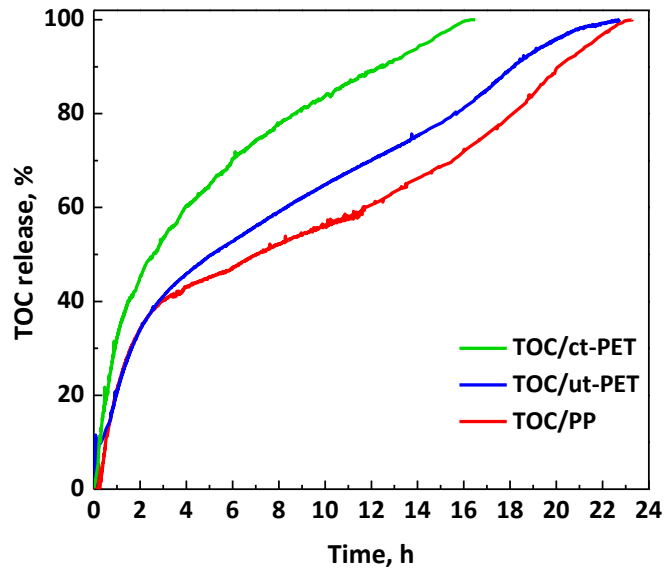
327 Table 1 Melting enthalpy (ΔH_m) and crystallinity degree (%) of pure and loaded films.

Sample	ΔH_m [J/g]	Crystallinity degree [%]
--------	-----------------------	--------------------------

unprocessed PP	88.97	42.98
TOC/PP	64.03	30.93
pure PET	42.15	30.10
ct-PET	34.71	24.79
ut-PET	39.83	28.45

328

329 The migration of TOC from the packaging films into the food simulant D1 [23] was studied using
330 UV–vis spectroscopy. Release profiles of TOC incorporated into the films, processed by
331 supercritical impregnation for 24 h, at 17 MPa and 40 °C, are shown in Figure 6. Unprocessed TOC
332 was wholly dissolved in the release medium in almost 45 minutes, whereas the release of TOC was
333 significantly delayed by its impregnation into films with SC-CO₂. In particular, all impregnated TOC
334 migrated in 16 h from corona discharge treated PET surface (ct-PET), whereas it took 22.8 h and
335 23.3 h respectively from untreated PET surface (ut-PET) and PP film, which showed the slowest
336 release profile. Release profiles revealed the presence of an initial burst-like effect, which was
337 about 10 % in case of PP and ut-PET and 20% for ct-PET, due to the percentage of TOC located
338 on/near the film surface, which dissolved quickly. In agreement with results about impregnation
339 kinetics, the faster release of TOC from ct-PET is related to the lower penetration of TOC into the
340 corona treated surface due to a low affinity with the additional polar groups formed during the
341 treatment.



342

343

Figure 6 Release kinetics of TOC in food simulant D1 from single-layer films.

344

3.3 Kinetics of TOC impregnation into multilayer PET/PP film

345

Since the best results, from the release kinetics point of view, were obtained considering TOC

346

release from PP film, the supercritical impregnation of TOC into a multilayer PET/PP film was

347

studied by exposing the PP surface to the TOC dissolved in SC-CO₂. Indeed, the use of PP/PET

348

multilayer film may be more favorable than the monolayer film. Indeed, the inner active layer (PP

349

in this specific case) allows the migration of the active compound (TOC) towards the food surface.

350

On the contrary, the outer layer (PET) is in contact with the external environment, offering more

351

protection for the active matrix layer and reducing the unwanted migration of the active

352

compound towards the outside of the package.

353

Even in the case of the multilayer film, the uptake (q_t) was expressed per unit area of film, as the

354

ratio between the amount of impregnated TOC per cm² of film ($\text{mg}_{\text{TOC}}/\text{cm}^2_{\text{FILM}}$). The impregnation

355

kinetics of TOC into a multilayer PET/PP film, reported in Figure 7, showed that the quantity of

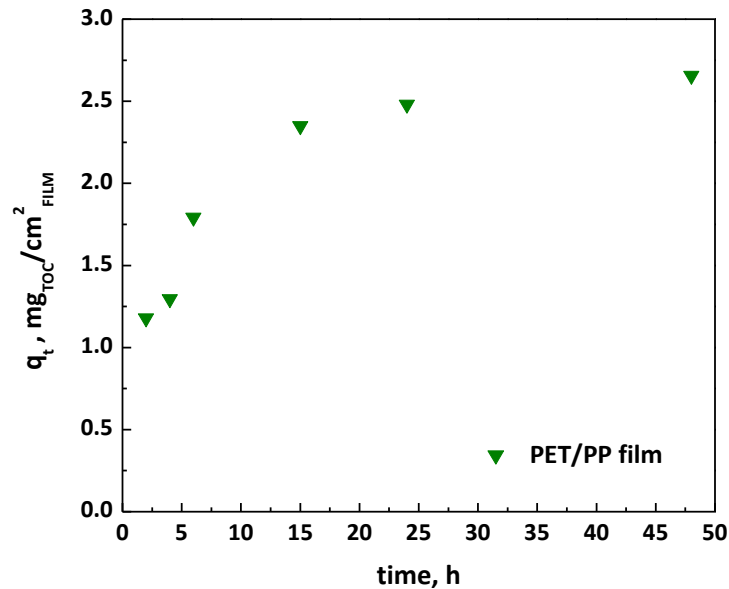
356

loaded TOC increased with the contact time, up to a maximum value reached in about 48 h equal

357

to 2.66 $\text{mg}_{\text{TOC}}/\text{cm}^2_{\text{FILM}}$. This maximum amount of TOC loaded in the multilayer film, in terms of

358 $\text{mg}_{\text{TOC}}/\text{cm}^2_{\text{FILM}}$, was similar to the one obtained using the monolayer PP film. From the kinetics
359 results, it is possible to deduce that a sufficient loading is reached after 24 h.



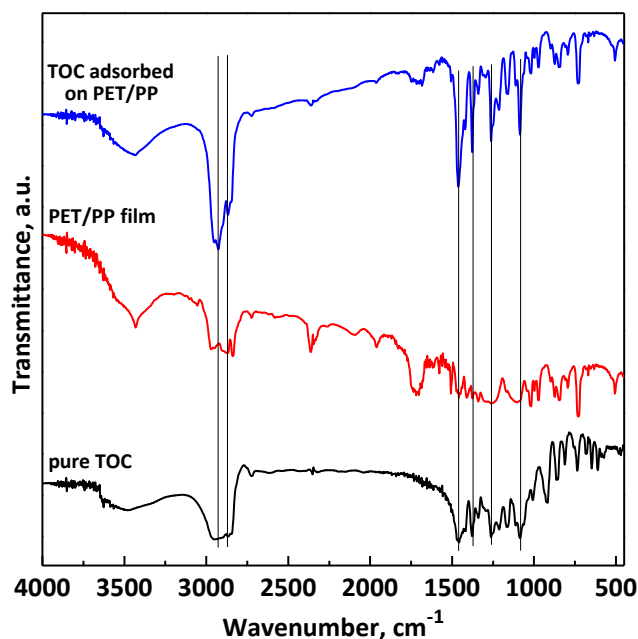
360

361 Figure 7 Kinetic curve at 17 MPa and 40 °C for the impregnation of TOC into multilayer PET/PP film.

362 3.4 Characterization of multilayer PET/PP films after impregnation

363 FT-IR spectra of pure TOC, pure multilayer PET/PP film, and TOC impregnated into multilayer
364 PET/PP film are reported in Figure 8. The spectrum of multilayer PET/PP film exhibited both the
365 characteristic peaks of monolayer PET and PP films. In addition to these, the spectra of the
366 impregnated sample showed the typical bands of TOC, such as the peaks at 2927 and 2868 cm^{-1}
367 related to the asymmetric and symmetric stretching vibrations of the CH_2 and CH_3 , at 1262 cm^{-1}
368 for CH_2 and at 1086 cm^{-1} for plane bending of phenyl [44]. Moreover, the presence of TOC was
369 confirmed by an increase of the absorbance peaks at 1378 and 1460 cm^{-1} , respectively associated
370 to the methyl symmetric and asymmetric bending [38], observed in the spectrum of loaded
371 multilayer PET/PP film with respect to the pure one. The percentage increase of the absorbance at
372 1378 and 1460 cm^{-1} was found to be about 79% and 83%, respectively. Moreover, the presence of
373 TOC peaks at 2927 and 2868 cm^{-1} was less evident in monolayer films, slightly noticeable in the

374 case of ut-PET monolayer film, while it is more accentuated in the spectrum of multilayer film, as
375 shown in Figure 8.



376

377 Figure 8 FT-IR spectra of pure TOC, pure multilayer PET/PP film and TOC impregnated into multilayer PET/PP film.

378

Vertical lines are referred to the peaks at 2927, 2868, 1460, 1378, 1262 and 1086 cm^{-1}

379

Migration tests of TOC in food simulant D1 were performed on multilayer PET/PP film to study its

380

possible use as active packaging. The release profile of TOC impregnated into PET/PP film (17 MPa,

381

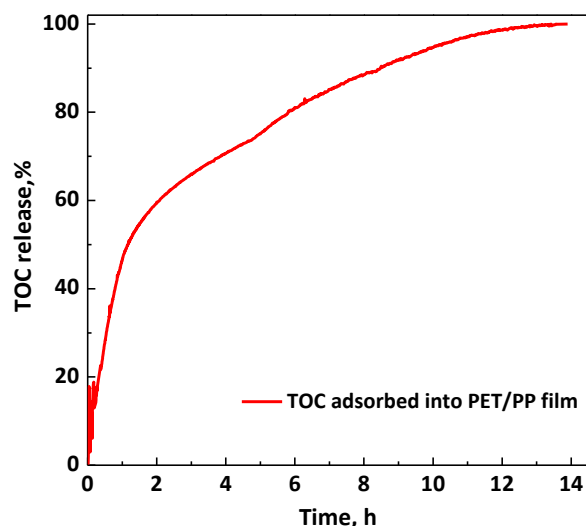
40 °C and 24 h) is reported in Figure 9. It is possible to observe that TOC completely migrated from

382

the multilayer film into food simulant D1 in 14 hours. . In conclusion, the impregnation with SC-

383

CO₂ into polymeric films has excellent potential to develop controlled-release packaging.



384

385 Figure 9 Release kinetics of TOC in food simulant D1 from multilayer PET/PP film.

386

387 The antioxidant activity was determined for unprocessed TOC, TOC impregnated on each
 388 monolayer (PP, ut-PET and ct-PET) and multilayer PET/PP films at 17 MPa and 40 °C for 24 h. An
 389 equivalent amount of TOC was considered to compare unprocessed TOC and impregnated films.

390 In particular, the antioxidant activity was checked to understand if TOC was damaged by thermal
 391 and oxidative degradation during the impregnation process. Results of percentage inhibition (%I)
 392 of the loaded films are similar to those of pure TOC, as demonstrated in Table 2 by reporting the
 393 data obtained after two hours of reaction with DPPH radical. Quantitatively, the reduction of the
 394 percentage inhibition with respect to the %I of unprocessed TOC was included between a
 395 minimum of 0.11 % for TOC impregnated into the ut-PET film to a maximum of 0.43 % for TOC
 396 loaded on PP film. These results confirmed that, in all cases, the antioxidant power of the active
 397 compound is preserved after the impregnation with SC-CO₂.

398

Table 2 Antioxidant activities in terms of percentage inhibition (%I) for pure TOC and loaded films.

Sample	%I
unprocessed TOC	92.4

PP	92.0
ct-PET	92.2
ut-PET	92.3
multilayer PET/PP	92.1

399

400 **4. Conclusions**

401 In the present work, the adsorption of TOC into polymeric films using supercritical impregnation
402 was studied, firstly considering single-layer PP and PET films and, then, multilayer PET/PP films.
403 The influence of corona discharge treatment on supercritical impregnation was also investigated
404 comparing the PET untreated surface with the treated one. PET surface with corona discharge
405 treatment showed the worst results both concerning the amount of impregnated TOC and the
406 release profile, whereas the attainment of TOC loaded into PP films was the best option to
407 produce a controlled-release packaging, with high values of loaded TOC. According to the
408 literature, the shifts of melting and glass transition temperatures of polymers was observed from
409 DSC analyses due to the well-known swelling and plasticizing effects of SC-CO₂ that allow a better
410 penetration of the active compound into the polymer substrate, resulting in high loadings. Based
411 on the results obtained for monolayers, to create active multilayer films, the impregnation of TOC
412 with SC-CO₂ was studied considering the PP surface of PET/PP film. Migration tests in food
413 simulant D1 (50% EtOH) demonstrated that the impregnation of TOC into polymeric films using SC-
414 CO₂ induced a prolonged release of the vitamin. These results are promising from an industrial
415 point of view, confirming the effectiveness of this process to produce controlled-release
416 packaging. Moreover, the antioxidant activity tests confirmed that the impregnation process did
417 not damage the TOC structure.

418 Besides, supercritical impregnation has proved to be an effective route to overcome the main
419 limitations associated with the production of active packaging with conventional techniques.
420 Indeed, high loading values, up to $3.20 \text{ mg}_{\text{TOC}}/\text{cm}^2_{\text{film}}$ and $2.66 \text{ mg}_{\text{TOC}}/\text{cm}^2_{\text{film}}$, for monolayer and
421 multilayer films respectively, were obtained. This result can be ascribed to the low temperature
422 used and to the high diffusivity of SC-CO₂, which allows to avoid the volatilization/degradation of
423 the active substance and, at the same time, to have a rapid penetration of the active principle into
424 the polymer matrix.

425 **Acknowledgments**

426 The authors thank Alessia De Lucia and Antonio Pecci for their help in carrying out part of the
427 experiments during their bachelor theses in chemical engineering at the University of Salerno. The
428 financial support of the Italian Ministry of Scientific Research is also acknowledged.

429 REFERENCES

- 430 [1] S. Concilio, P. Iannelli, L. Sessa, R. Olivieri, A. Porta, F. De Santis, R. Pantani, S. Piotto, Biodegradable
431 antimicrobial films based on poly (lactic acid) matrices and active azo compounds, *J. Appl. Pol. Sci.* 132(33)
432 (2015).
- 433 [2] L. Di Maio, F. Marra, A. Apicella, L. Incarnato, Evaluation and modeling of scavenging performances of
434 active multilayer PET based films for food preservation, *Chem. Eng. Trans.* 57 (2017) 1879-1884.
- 435 [3] N.D. Kruijf, M.V. Beest, R. Rijk, T. Sipiläinen-Malm, P.P. Losada, B.D. Meulenaer, Active and intelligent
436 packaging: applications and regulatory aspects, *Food Addit. Contam.* 19(S1) (2002) 144-162.
- 437 [4] P. Franco, B. Aliakbarian, P. Perego, E. Reverchon, I. De Marco, Supercritical Adsorption of Quercetin on
438 Aerogels for Active Packaging Applications, *Ind. Eng. Chem. Res.* 57(44) (2018) 15105-15113.
- 439 [5] A.A. Nwakaudu, M.S. Nwakaudu, C.I. Owuamanam, N.C. Iheaturu, The use of natural antioxidant active
440 packaging films for food preservation, *Applied Signals Reports* 2(4) (2015) 38-50.
- 441 [6] E. Chiellini, *Environmentally compatible food packaging*, Elsevier, 2008.
- 442 [7] L.-N. Sun, L.-X. Lu, X.-L. Qiu, Y.-L. Tang, Development of low-density polyethylene antioxidant active films
443 containing α -tocopherol loaded with MCM-41 (Mobil Composition of Matter No. 41) mesoporous silica,
444 *Food Control* 71 (2017) 193-199.
- 445 [8] N. Gargiulo, I. Attianese, G.G. Buonocore, D. Caputo, M. Lavorgna, G. Mensitieri, M. Lavorgna, α -
446 Tocopherol release from active polymer films loaded with functionalized SBA-15 mesoporous silica,
447 *Microporous Mesoporous Mater.* 167 (2013) 10-15.
- 448 [9] P. Scarfato, E. Avallone, M.R. Galdi, L. Di Maio, L. Incarnato, Preparation, characterization, and oxygen
449 scavenging capacity of biodegradable α -tocopherol/PLA microparticles for active food packaging
450 applications, *Polym. Compos.* 38(5) (2017) 981-986.
- 451 [10] M.J. Fabra, A. López-Rubio, J.M. Lagaron, Use of the electrohydrodynamic process to develop
452 active/bioactive bilayer films for food packaging applications, *Food Hydrocoll.* 55 (2016) 11-18.
- 453 [11] N. Burgos, A.C. Mellinas, E. García-Serna, A. Jiménez, Nanoencapsulation of flavor and aromas in food
454 packaging, *Food Packaging*, Elsevier, 2017, pp. 567-601.
- 455 [12] V. Prosapio, E. Reverchon, I. De Marco, Incorporation of liposoluble vitamins within PVP microparticles
456 using supercritical antisolvent precipitation, *J. CO2 Util.* 19 (2017) 230-237.
- 457 [13] Y. Wu, Y. Qin, M. Yuan, L. Li, H. Chen, J. Cao, J. Yang, Characterization of an antimicrobial poly (lactic
458 acid) film prepared with poly (ϵ -caprolactone) and thymol for active packaging, *Polymers for Advanced
459 Technologies* 25(9) (2014) 948-954.
- 460 [14] S. Milovanovic, G. Hollermann, C. Errenst, J. Pajnik, S. Frerich, S. Kroll, K. Rezwan, J. Ivanovic,
461 Supercritical CO₂ impregnation of PLA/PCL films with natural substances for bacterial growth control in food
462 packaging, *Food Res. Int.* 107 (2018) 486-495.
- 463 [15] G. Caputo, M. Scognamiglio, I. De Marco, Nimesulide adsorbed on silica aerogel using supercritical
464 carbon dioxide, *Chem. Eng. Res. Des.* 90(8) (2012) 1082-1089.
- 465 [16] C. García-González, I. Smirnova, Use of supercritical fluid technology for the production of tailor-made
466 aerogel particles for delivery systems, *J. Supercrit. Fluids* 79 (2013) 152-158.
- 467 [17] L. Baldino, M. Sarno, S. Cardea, S. Irusta, P. Ciambelli, J. Santamaria, E. Reverchon, Formation of
468 cellulose acetate-graphene oxide nanocomposites by supercritical CO₂ assisted phase inversion, *Ind. Eng.
469 Chem. Res.* 54(33) (2015) 8147-8156.
- 470 [18] C. Daniel, S. Longo, S. Cardea, J.G. Vitillo, G. Guerra, Monolithic nanoporous-crystalline aerogels based
471 on PPO, *RSC Advances* 2(31) (2012) 12011-12018.
- 472 [19] I. Kikic, F. Vecchione, Supercritical impregnation of polymers, *Curr. Opin. Solid State Mater. Sci.* 7(4-5)
473 (2003) 399-405.
- 474 [20] A. Rojas, D. Cerro, A. Torres, M.J. Galotto, A. Guarda, J. Romero, Supercritical impregnation and kinetic
475 release of 2-nonanone in LLDPE films used for active food packaging, *J. Supercrit. Fluids* 104 (2015) 76-84.
- 476 [21] G.R. Medeiros, S.R. Ferreira, B.A. Carciofi, High pressure carbon dioxide for impregnation of clove
477 essential oil in LLDPE films, *Innov. Food Sci. Emerg.* 41 (2017) 206-215.

478 [22] C. Villegas, A. Torres, M. Rios, A. Rojas, J. Romero, C.L. de Dicastillo, X. Valenzuela, M.J. Galotto, A.
479 Guarda, Supercritical impregnation of cinnamaldehyde into polylactic acid as a route to develop
480 antibacterial food packaging materials, *Food Res. Int.* 99 (2017) 650-659.

481 [23] M. Belizón, M. Fernández-Ponce, L. Casas, C. Mantell, E.M. de la Ossa-Fernández, Supercritical
482 impregnation of antioxidant mango polyphenols into a multilayer PET/PP food-grade film, *J. CO2 Util.* 25
483 (2018) 56-67.

484 [24] C. Cejudo Bastante, L. Casas Cardoso, C. Mantell Serrano, E.J. Martínez de la Ossa, Supercritical
485 impregnation of food packaging films to provide antioxidant properties, *J. Supercrit. Fluids* 128 (2017) 200-
486 207.

487 [25] E.A. Decker, R.J. Elias, D.J. McClements, *Oxidation in foods and beverages and antioxidant applications: management in different industry sectors*, Elsevier, 2010.

488 [26] R. Campardelli, E. Reverchon, α -Tocopherol nanosuspensions produced using a supercritical assisted
489 process, *J. Food Eng.* 149 (2015) 131-136.

490 [27] M.d.M. Castro López, S. Dopico García, A. Ares Pernas, J.M. López Vilariño, M.V. González Rodríguez,
491 Effect of PPG-PEG-PPG on the tocopherol-controlled release from films intended for food-packaging
492 applications, *J. Agric. Food Chem.* 60(33) (2012) 8163-8170.

493 [28] X. Chen, D.S. Lee, X. Zhu, K.L. Yam, Release kinetics of tocopherol and quercetin from binary
494 antioxidant controlled-release packaging films, *J. Agric. Food Chem.* 60(13) (2012) 3492-3497.

495 [29] I. Siró, É. Fenyvesi, L. Szenté, B. De Meulenaer, F. Devlieghere, J. Orgoványi, J. Sényi, J. Barta, Release of
496 α -tocopherol from antioxidative low-density polyethylene film into fatty food simulant: influence of
497 complexation in beta-cyclodextrin, *Food Addit. Contam.* 23(8) (2006) 845-853.

498 [30] S.W. Hwang, J.K. Shim, S.E. Selke, H. Soto-Valdez, L. Matuana, M. Rubino, R. Auras, Poly (L-lactic acid)
499 with added α -tocopherol and resveratrol: optical, physical, thermal and mechanical properties, *Polym. Int.*
500 61(3) (2012) 418-425.

501 [31] I. De Marco, E. Reverchon, Starch aerogel loaded with poorly water-soluble vitamins through
502 supercritical CO₂ adsorption, *Chem. Eng. Res. Des.* 119 (2017) 221-230.

503 [32] Y. Yokozaki, Y. Shimoyama, Loading of vitamin E into silicone hydrogel by supercritical carbon dioxide
504 impregnation toward controlled release of timolol maleate, *J. Supercrit. Fluids* 131 (2018) 11-18.

505 [33] G. Barbaro, M.R. Galdi, L. Di Maio, L. Incarnato, Effect of BOPET film surface treatments on adhesion
506 performance of biodegradable coatings for packaging applications, *European Polymer Journal* 68 (2015) 80-
507 89.

508 [34] J.M. Goddard, J. Hotchkiss, Polymer surface modification for the attachment of bioactive compounds,
509 *Progress in polymer science* 32(7) (2007) 698-725.

510 [35] I. Smirnova, J. Mamic, W. Arlt, Adsorption of drugs on silica aerogels, *Langmuir* 19(20) (2003) 8521-
511 8525.

512 [36] Y. Zhang, D. Kang, M. Aindow, C. Erkey, Preparation and characterization of ruthenium/carbon aerogel
513 nanocomposites via a supercritical fluid route, *J. Phys. Chem. B* 109(7) (2005) 2617-2624.

514 [37] E. Bender, Equation of State Exactly Representing The Phase Behaviors of Pure Substances, *Proc. 5th*
515 *Symp. Thermophys. Prop. Am. Soc. Mech. Eng.* (1970) 227-235.

516 [38] J. Gulmine, P. Janissek, H. Heise, L. Akcelrud, Polyethylene characterization by FTIR, *Polymer Testing*
517 21(5) (2002) 557-563.

518 [39] A.S.f. Testing, Materials, Standard test method for transition temperatures and enthalpies of fusion
519 and crystallization of polymers by differential scanning calorimetry, ASTM International, 2015.

520 [40] EU, European Regulation EU 10-2011 for Plastics Intended to come into Contact with Food, (2011).

521 [41] W. Brand-Williams, M.-E. Cuvelier, C. Berset, Use of a free radical method to evaluate antioxidant
522 activity, *LWT-Food science and Technology* 28(1) (1995) 25-30.

523 [42] S. Areerat, E. Funami, Y. Hayata, D. Nakagawa, M. Ohshima, Measurement and prediction of diffusion
524 coefficients of supercritical CO₂ in molten polymers, *Polymer Engineering & Science* 44(10) (2004) 1915-
525 1924.

526 [43] W.J. Weber, J.C. Morris, Kinetics of adsorption on carbon from solution, *Journal of the Sanitary*
527 *Engineering Division* 89(2) (1963) 31-60.

- 529 [44] S.D. Silva, N.F. Rosa, A.E. Ferreira, L.V. Boas, M.R. Bronze, Rapid determination of α -tocopherol in
530 vegetable oils by fourier transform infrared spectroscopy, *Food Anal. Methods* 2(2) (2009) 120-127.
- 531 [45] S. Rodríguez-Llamazares, Polypropylene/starch blends: Study of thermal and morphological properties,
532 *J. Chil. Chem. Soc.* 58(1) (2013) 1643-1646.
- 533 [46] M. Jarrigeon, B. Chabert, D. Chatain, C. Lacabanne, G. Nemoz, Multiple transitions in isotactic
534 polypropylene around and above the glass transition, *Journal of Macromolecular Science, Part B: Physics*
535 17(1) (1980) 1-24.
- 536 [47] A. Apicella, P. Scarfato, L. Di Maio, E. Garofalo, L. Incarnato, Preparation and performance analysis of
537 active packaging PET films combining oxygen scavenging with barrier properties for shelf life extension of
538 sensitive foods, *J. Appl. Packag. Res.* 10(2) (2018) 1-8.
- 539 [48] Z. Lian, S.A. Epstein, C.W. Blenk, A.D. Shine, Carbon dioxide-induced melting point depression of
540 biodegradable semicrystalline polymers, *J. Supercrit. Fluids* 39(1) (2006) 107-117.
- 541 [49] E. Oral, K.K. Wannomae, N. Hawkins, W.H. Harris, O.K. Muratoglu, α -Tocopherol-doped irradiated
542 UHMWPE for high fatigue resistance and low wear, *Biomaterials* 25(24) (2004) 5515-5522.
- 543 [50] L.T. Sin, S.-T. Bee, T.-T. Tee, A.A.H. Kadhum, C. Ma, A. Rahmat, P. Veerasamy, Characterization of α -
544 tocopherol as interacting agent in polyvinyl alcohol–starch blends, *Carbohydr. Polym.* 98(2) (2013) 1281-
545 1287.
- 546
- 547